

Comparison of thermal annealing effects on electrical activation of MBE grown and ion implant Si-doped In_{0.53}Ga_{0.47}As

Aaron G. Lind, Henry L. Aldridge Jr., Cory C. Bomberger, Christopher Hatem, Joshua M. O. Zide, and Kevin S. Jones

Citation: *Journal of Vacuum Science & Technology B* **33**, 021206 (2015); doi: 10.1116/1.4914319

View online: <http://dx.doi.org/10.1116/1.4914319>

View Table of Contents: <http://scitation.aip.org/content/avs/journal/jvstb/33/2?ver=pdfcov>

Published by the AVS: Science & Technology of Materials, Interfaces, and Processing

Articles you may be interested in

[Concentration-dependent diffusion of ion-implanted silicon in In_{0.53}Ga_{0.47}As](#)

Appl. Phys. Lett. **105**, 042113 (2014); 10.1063/1.4892079

[Electrically active Er doping in InAs, In_{0.53}Ga_{0.47}As, and GaAs](#)

Appl. Phys. Lett. **101**, 232103 (2012); 10.1063/1.4769248

[Electrical properties of Er-doped In_{0.53}Ga_{0.47}As](#)

J. Vac. Sci. Technol. B **29**, 03C117 (2011); 10.1116/1.3559480

[InSb_{1-x}N_x/InSb/GaAs alloys by thermal annealing for midinfrared photodetection](#)

Appl. Phys. Lett. **97**, 221112 (2010); 10.1063/1.3524228

[Heavily carbon-doped In_{0.53}Ga_{0.47}As on InP \(001\) substrate grown by solid source molecular beam epitaxy](#)

J. Vac. Sci. Technol. B **17**, 1190 (1999); 10.1116/1.590721

 **SHIMADZU** Excellence in Science **Powerful, Multi-functional UV-Vis-NIR and FTIR Spectrophotometers**

Providing the utmost in sensitivity, accuracy and resolution for applications in materials characterization and nano research

- Photovoltaics
- Polymers
- Thin films
- Paints
- Ceramics
- DNA film structures
- Coatings
- Packaging materials

[Click here to learn more](#)



Comparison of thermal annealing effects on electrical activation of MBE grown and ion implant Si-doped $\text{In}_{0.53}\text{Ga}_{0.47}\text{As}$

Aaron G. Lind^{a)} and Henry L. Aldridge, Jr.

Department of Materials Science and Engineering, University of Florida, Gainesville, Florida 32611

Cory C. Bomberger

Department of Materials Science and Engineering, University of Delaware, Newark, Delaware 19716

Christopher Hatem

Applied Materials, Gloucester, Massachusetts 01930

Joshua M. O. Zide

Department of Materials Science and Engineering, University of Delaware, Newark, Delaware 19716

Kevin S. Jones

Department of Materials Science and Engineering, University of Florida, Gainesville, Florida 32611

(Received 14 November 2014; accepted 24 February 2015; published 6 March 2015)

The effect of thermal annealing on the net donor concentration and diffusion of Si in $\text{In}_{0.53}\text{Ga}_{0.47}\text{As}$ is compared for electrically active layers formed by ion implantation versus molecular beam epitaxy (MBE). Upon thermal treatment at temperatures of 700 °C or higher for 10 min, both ion implanted and growth-doped substrates converge to a common net donor solubility. These results indicate that while MBE doped substrates typically exhibit higher active concentrations relative to implanted substrates, the higher active Si concentrations from MBE growth are metastable and susceptible to deactivation upon subsequent thermal treatments after growth. Active Si doping concentrations in MBE doped material and ion-implanted materials are shown to converge toward a fixed net donor solubility limit of $1.4 \times 10^{19} \text{ cm}^{-3}$. Secondary ion mass spectroscopy of annealed samples indicates that the diffusivity of Si in MBE doped substrates is higher than those of ion implanted substrates presumably due to concentration-dependent diffusion effects. © 2015 American Vacuum Society. [<http://dx.doi.org/10.1116/1.4914319>]

I. INTRODUCTION

There is a great deal of interest in using III–V materials and, in particular, InGaAs, for future generations of CMOS devices given the much higher electron mobilities of these materials over Si.¹ One challenge to adoption of these materials in future n-channel devices is the low reported n-type dopant solubilities in InGaAs, which is a significant inhibitor to the creation of low resistance source/drain regions and ohmic contacts.² Reported maximum net donor solubilities of grown-in dopants regularly show higher doping concentrations than are achievable for implanted dopants in III–V materials, leading previous authors to conclude that residual implant damage after activating anneals was the likely reason for reduced net donor solubility from implants relative to grown in dopants.^{3–6} However, more recent studies have called into question the previously advanced theories.^{7,8} Understanding the stability of grown in Si dopants in III–V materials is also technologically relevant due to the desire to integrate III–V transistors with existing Si transistor technologies for system on a chip (SoC) designs that generally require much higher processing temperatures. The goal of these experiments was to directly compare activation and deactivation, as well as the diffusion behavior, for implanted and grown in Si dopants in InGaAs.

II. EXPERIMENT

Two types of substrates were used in this study. Implanted substrates consisted of a nonamorphizing 10 keV, $5 \times 10^{14} \text{ cm}^{-2}$ Si⁺ implant performed at 80 °C into 300 nm of metalorganic chemical vapor deposition-grown $\text{In}_{0.53}\text{Ga}_{0.47}\text{As}$ on semi-insulating InP. Grown in substrates consisted of 380 nm of molecular beam epitaxy (MBE) $\text{In}_{0.53}\text{Ga}_{0.47}\text{As}$ grown at 490 °C on semi-insulating InP with the top 60 nm of the MBE $\text{In}_{0.53}\text{Ga}_{0.47}\text{As}$ structure being Si doped to a concentration of $7 \times 10^{19} \text{ cm}^{-3}$. All samples were then encapsulated with 15 nm of Al_2O_3 by atomic layer deposition at 250 °C to protect against surface degradation upon subsequent thermal treatments. Samples of growth-doped and implant-doped substrates of 15 × 15 mm were annealed side-by-side at 550, 600, 650, 700, and 750 °C in Ar ambient in a tube furnace for 10 min. Buffered oxide etch was used to remove the dielectric encapsulant prior to secondary ion mass spectroscopy (SIMS) and electrical characterization with Van der Pauw Hall effect using pressed on indium contacts.

III. RESULTS AND DISCUSSION

Figure 1 shows the postanneal Si profiles for MBE grown Si doped $\text{In}_{0.53}\text{Ga}_{0.47}\text{As}$. Significant Si diffusion is observed for anneals of 700 °C or greater while anneals performed much closer to the 490 °C growth temperature (550–650 °C) exhibit nearly coincident Si concentration profiles. The

^{a)}Electronic mail: aglind@ufl.edu

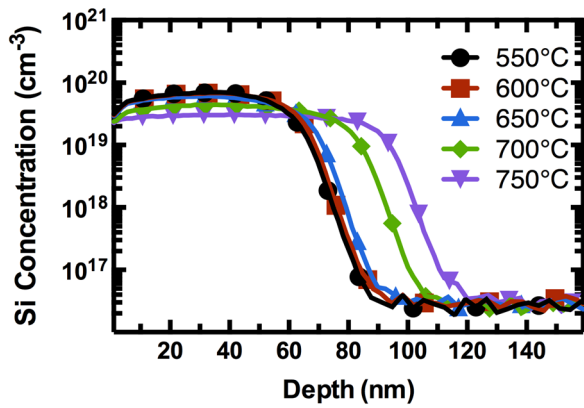


FIG. 1. (Color online) Postanneal SIMS profiles for Si-doped, MBE-grown $\text{In}_{0.53}\text{Ga}_{0.47}\text{As}$ after 10 m furnace anneals at 550, 600, 650, 700, and 750 °C.

observed peak Si concentration for anneals at 550–600 °C is approximately $7 \times 10^{19} \text{ cm}^{-3}$. After annealing at 750 °C, the total chemical solubility indicated by the plateau concentration of Si is reduced to $3 \times 10^{19} \text{ cm}^{-3}$. SIMS profiles of post-anneal Si in implant-doped substrates shown in Fig. 2 exhibit similar trends with the MBE grown samples with anneals of 750 °C showing significant diffusion. Implanted Si diffusion at 750 and 700 °C is less pronounced in this work compared with our previous work⁹ despite the same implant conditions and annealing times. The discrepancy between these reports is attributed to differences in the measured and actual sample annealing temperatures between the two experiments. This makes absolute comparisons between the two experiments difficult. However, the side-by-side annealing of the MBE and implanted substrates in this work ensures that the postanneal SIMS and measured electrical activation are self-consistent. As such, meaningful comparisons can be made between growth-doped and implant doped samples for given annealing conditions.

The observed chemical solubility of Si of $3 \times 10^{19} \text{ cm}^{-3}$ for anneals performed at 750 °C on both implant and growth doped substrates is consistent with our recent report⁹ of highly concentration dependent diffusion of Si in $\text{In}_{0.53}\text{Ga}_{0.47}\text{As}$ for concentrations above $3 \times 10^{19} \text{ cm}^{-3}$. This result suggests that the diffusion mechanism is similar in

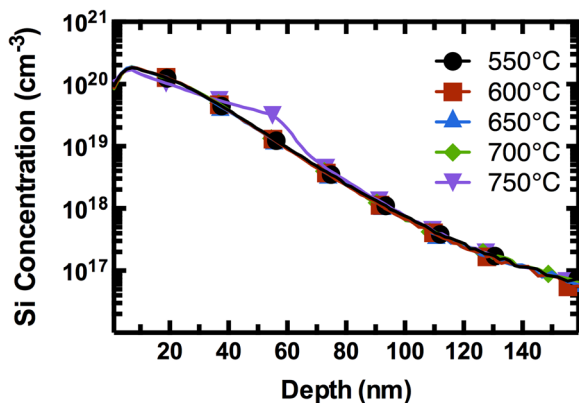


FIG. 2. (Color online) Postanneal SIMS profiles for 10 keV $5 \times 10^{14} \text{ cm}^{-2}$ Si^+ implants into $\text{In}_{0.53}\text{Ga}_{0.47}\text{As}$ after 10 m furnace anneals at 550, 600, 650, 700, and 750 °C.

both the implant doped and growth doped material. Si diffusion in the epitaxially doped substrates is more pronounced for anneals performed at 700 and 750 °C than for implanted dopants. The effective diffusivities, which comprised both concentration-dependent and Fickian components of diffusion after annealing at 750 °C were calculated from post-anneal SIMS and indicate that the total Si diffusivity is approximately eight times higher for epitaxially incorporated Si relative to implanted Si ($D_{\text{eff(MBE)}} = 7.1 \times 10^{-13} \text{ cm}^2 \text{ s}^{-1}$, $D_{\text{eff(Implant)}} = 5.9 \times 10^{-14} \text{ cm}^2 \text{ s}^{-1}$). These diffusivity values were obtained by implementing a $\text{Si}_{\text{III}}\text{-V}_{\text{III}}$ pair model in Florida object oriented process simulator in which concentration effects were accounted for by using Poisson's equation with a net active donor concentration set at $1.4 \times 10^{19} \text{ cm}^{-3}$ and a mobile concentration at $3 \times 10^{19} \text{ cm}^{-3}$. As-implanted excess vacancy and interstitial profiles were predicted using the transport of ions in matter to account for damage effects in ion implanted samples. Previous work has shown that Si diffusion in InGaAs is heavily concentration dependent⁸ and previous studies of concentration dependent Si diffusion in GaAs have shown that substrates with higher background electrically active donor concentrations exhibit higher Si diffusivity.^{10,11} The enhanced diffusivity observed in MBE doped substrates relative to implanted substrates in this study is also consistent with reports of Fermi-level effects on Si diffusion in InGaAs (Ref. 12) as MBE doped substrates exhibit much higher initial active donor concentrations.

Figure 3 shows the measured sheet number (N_s). Implanted samples exhibit a steady improvement in N_s with increasing anneal temperature while grown-in Si dopants show a decrease in N_s upon annealing at temperature up to 650 °C. The observed increase in N_s for growth-doped substrates annealed at temperatures of 700 °C and above can be attributed to diffusion of Si further into the bulk of the material, resulting in an increase in the depth of the electrically active layer as evidenced by the SIMS in Fig. 1. Postanneal net donor concentrations were calculated from the postanneal SIMS and N_s measurements using the methodology described elsewhere,^{13,14} to compare the active donor concentration. Figure 4 shows the calculated net donor solubility as a function of annealing temperature. As-grown, epitaxially doped InGaAs,

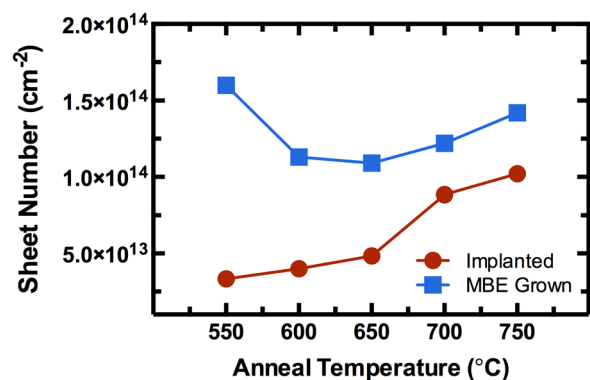


FIG. 3. (Color online) Active sheet number (N_s) of Si^+ -implanted and MBE Si-doped $\text{In}_{0.53}\text{Ga}_{0.47}\text{As}$ specimens as a function of annealing temperature after 10 m furnace anneals at 550, 600, 650, 700, and 750 °C.

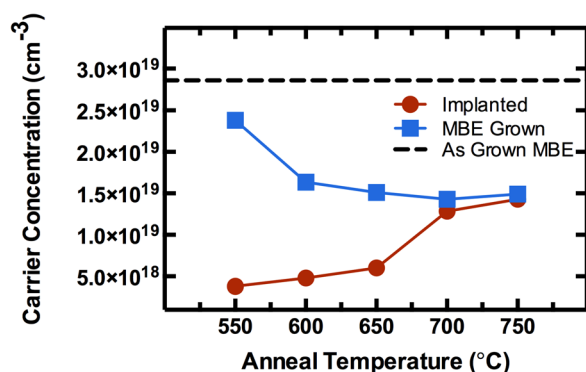


FIG. 4. (Color online) Calculated net donor concentration (N) of Si^+ -implanted and MBE Si-doped $\text{In}_{0.53}\text{Ga}_{0.47}\text{As}$ specimens as a function of annealing temperature after 10 min furnace anneals at 550, 600, 650, 700, and 750 °C.

indicated by the dashed line in Fig. 4, exhibits a calculated active donor concentration of $2.86 \times 10^{19} \text{ cm}^{-3}$, which is consistent with previous reports of maximum active donor solubilities of $3\text{--}6 \times 10^{19} \text{ cm}^{-3}$.^{15–18} The calculated active concentration of grown-in Si in is shown to steadily decrease until annealing at 700 and 750 °C upon subsequent thermal treatments and stabilizes at $\approx 1.4 \times 10^{19} \text{ cm}^{-3}$ for anneals above 700 °C. Doping by ion implantation requires subsequent thermal treatment to move Si onto lattice sites and anneal damage created during implantation. Accounting for diffusion, the active donor concentration for implant-doped $\text{In}_{0.53}\text{Ga}_{0.47}\text{As}$ increases up to $1.4 \times 10^{19} \text{ cm}^{-3}$. This level of activation is the same as observed for grown-in electrically active layers after annealing for 10 min at temperatures above 700 °C as shown in Fig. 4, which suggests that annealing at temperatures ≥ 700 °C is sufficient to recover implant damage and cause the migration of implanted Si onto lattice sites. Despite previous reports generally concluding that the Si solubility in epitaxially doped $\text{In}_{0.53}\text{Ga}_{0.47}\text{As}$ was higher than that in implanted $\text{In}_{0.53}\text{Ga}_{0.47}\text{As}$, the results presented here indicate that the active donor concentration of both implant and grown in doping converge to the same limit of $1.4 \times 10^{19} \text{ cm}^{-3}$ after thermal treatments of 700–750 °C for 10 min. These anneals are shown to maximize the observed activation in implanted material and are further shown to be sufficient to cause Si diffusion. It is also worth noting that, in all annealing conditions where diffusion is observed, the active donor concentration is considerably less than the mobile chemical concentration, suggesting the presence of mobile, yet inactive or electrically compensated Si in $\text{In}_{0.53}\text{Ga}_{0.47}\text{As}$. *Ab initio* studies of Si dopants in GaAs have concluded that the formation of vacancy defects such as the $(\text{V}_{\text{Ga}})^{3-}$ or $(\text{Si}_{\text{Ga}}\text{V}_{\text{Ga}})^{2-}$ are energetically favorable at high Si concentrations and that Si diffusion likely occurs via a group III vacancy mechanism.^{19,20} The presence of the vacancy defects at high doping levels may help explain the difference between the mobile Si concentration ($>3 \times 10^{19} \text{ cm}^{-3}$) and the active donor concentration ($1.4 \times 10^{19} \text{ cm}^{-3}$) of Si in $\text{In}_{0.53}\text{Ga}_{0.47}\text{As}$. The discrepancy between the active concentration of ($1.4 \times 10^{19} \text{ cm}^{-3}$) and the plateau concentration of ($3 \times 10^{19} \text{ cm}^{-3}$), below which Si shows limited diffusion, may indicate that Si donor

compensation between 1.4×10^{19} and $3 \times 10^{19} \text{ cm}^{-3}$ is the result of either Si configurations that have very limited diffusivity relative to the $(\text{Si}_{\text{Ga}}\text{V}_{\text{Ga}})^{2-}$ complex, such as neutral Si–Si next-nearest neighbor pairs or Si_{As} acceptor type defects, or due to rapid formation and dissolution of dopant-defect complexes in which dopants are mobile only during brief periods when they are uncomplexed.

Mobility (Fig. 5) decreases with increasing annealing temperature from 550 to 700 °C in the case of implanted material as expected from the increase in ionized impurity scattering. In contrast, the mobility of grown in $\text{In}_{0.53}\text{Ga}_{0.47}\text{As}$ As increases with annealing temperature due to a decrease in ionized impurity scattering as the net donor concentration decreases (Fig. 4). For anneals of 700–750 °C, the measured mobility of both growth doped and implant doped materials is shown to be nearly coincident as is expected from the net donor solubilities and subsequent contribution to mobility due to ionized impurity scattering.

Most reports of Si implants in to $\text{In}_{0.53}\text{Ga}_{0.47}\text{As}$ (Refs. 4, 5, 8, 14, 21, and 22) show active donor concentrations lower than the maximum reported active donor concentration for grown-in dopants, but the reasons for this difference have been mostly speculative. Authors generally suggest that damage created from implantation, or in the case of Si, the amphoteric nature tends to limit the net donor solubility. The results presented in this work suggest that the differences in observed active donor concentrations is simply a result of the differences in processing required to activate dopants in epitaxially grown material versus implant doped material. In the case of epitaxial doping, dopants are incorporated directly onto lattice sites while diffusion of atoms from interstitial sites onto lattice sites is required to achieve activation in the case of nonamorphizing implants. A precipitous drop in activation is observed from the as-grown condition for anneals at 550 and 600 °C, with deactivation converging to a constant $1.4 \times 10^{19} \text{ cm}^{-3}$ level for anneals above 650 °C. This deactivation coincides with the onset of diffusion in the grown-in Si doped layers implying that diffusion of Si results in a fixed active donor concentration of $1.4 \times 10^{19} \text{ cm}^{-3}$. Similarly, limited Si activation upon diffusion is also seen for the ion-implanted case. The results of this work suggest that the

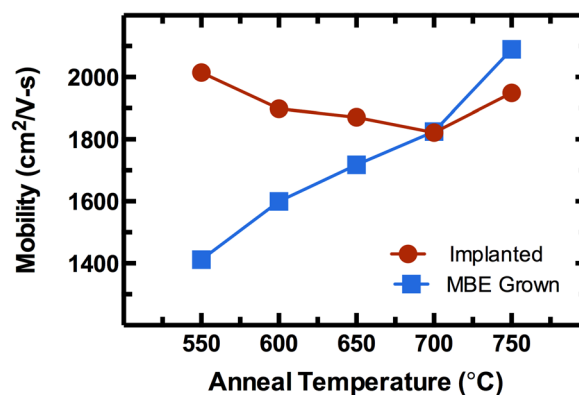


FIG. 5. (Color online) Mobility (μ) of Si^+ -implanted and MBE Si-doped $\text{In}_{0.53}\text{Ga}_{0.47}\text{As}$ specimens as a function of annealing temperature after 10 min furnace anneals at 550, 600, 650, 700, and 750 °C.

active Si concentration in epitaxially grown $\text{In}_{0.53}\text{Ga}_{0.47}\text{As}$ is metastable in instances where the incorporated Si concentrations are above $1.4 \times 10^{19} \text{cm}^{-3}$. Deactivation of MBE doped Si grown at 490°C was observed after annealing at 550°C for 10 min. This suggests that annealing at temperatures above the growth temperature can result in deactivation. One possible reason for some of the observed variation in reported maximum net donor solubility limits in growth doped material might be the differences in growth temperatures as the results of this work would suggest that lower growth temperatures are expected to show higher active sheet numbers so long as other growth-related issues are avoided.^{15–18}

Watanabe *et al.* observed deactivation of Si in InGaAs to a net active concentration of $1.6 \times 10^{19} \text{cm}^{-3}$ after 10 min anneals at temperatures above 700°C in agreement with the results of this work, but the measured deactivation was attributed to the diffusion of Si into the underlying substrate.²² We present evidence of deactivation well before the onset of significant diffusion in growth doped $\text{In}_{0.53}\text{Ga}_{0.47}\text{As}$, indicating that the resultant deactivation observed by Watanabe *et al.* cannot be fully explained by diffusion into the underlying substrate. Instead, the resultant deactivation behavior in growth-doped substrates and the common ultimate activation limit are consistent with the formation of electrically compensating native defects as proposed by Walukiewicz,^{23,24} which suggests that the maximum achievable solubility of a given dopant will be intrinsic to the doped material. The application of these results has further implications for understanding the potential effectiveness of the more recently developed monolayer doping technique in III–V materials. Monolayer doping has been used to successfully dope Si into $\text{In}_{0.53}\text{Ga}_{0.47}\text{As}$ and create very abrupt profiles, but the technology relies on the equilibrium diffusion of dopants from the surface of a material into the bulk.^{25–27} The results presented in this work suggest that it will be difficult to achieve active doping concentrations greater than $1.4 \times 10^{19} \text{cm}^{-3}$ as the compensating mechanisms resulting in limited activation appear to form well before significant diffusion can occur and profiles that show measurable Si diffusion result in limited active donor concentrations of $1.4 \times 10^{19} \text{cm}^{-3}$ regardless of whether dopants were incorporated via ion implantation or during growth. Design of future CMOS devices that integrate Si doped $\text{In}_{0.53}\text{Ga}_{0.47}\text{As}$ with existing Si and Ge technologies will require careful consideration of the effects that subsequent thermal processing may have on the electrical activation and diffusion of Si. For example, many current techniques of contact formation require high temperature annealing of refractory metals such as Pt, Pd, and Mo to form ohmic contacts which could further deactivate the underlying electrically active layers in as-grown material.^{28–31}

IV. SUMMARY AND CONCLUSION

In conclusion, it has been shown that subsequent thermal treatment of epitaxially grown Si-doped layers of $\text{In}_{0.53}\text{Ga}_{0.47}\text{As}$ above the temperatures at which growth occurred results in deactivation toward the same observed

maximum net donor concentration of $1.4 \times 10^{19} \text{cm}^{-3}$ for implanted materials, suggesting the presence of a common crystal thermodynamic limit to Si doping in InGaAs substrates. It is also shown that the Si diffusion in heavily doped MBE substrates is higher than that observed in implanted substrates, presumably due to concentration dependent diffusion effects. The concentration dependent diffusion and apparent Si solubility of $3 \times 10^{19} \text{cm}^{-3}$, observed for both implanted and MBE substrates, is consistent with the concentration dependent diffusion behavior observed in previous experiments of implanted Si in InGaAs . In order to maintain the increased dopant incorporation afforded by the nonequilibrium incorporation of Si into $\text{In}_{0.53}\text{Ga}_{0.47}\text{As}$ by epitaxial growth methods, annealing above the growth temperature must be minimized. This result has important implications for the design and production of future CMOS devices where multiple thermal treatments at differing temperatures will be required for processing disparate material types in a single device.

ACKNOWLEDGMENTS

The authors acknowledge the Semiconductor Research Corporation for funding this work. C. C. Bomberger was supported primarily by the NSF (DMR-1105137). The authors would also like to further acknowledge the valuable feedback from reviewers, which has improved the quality of this manuscript.

¹M. Heyns and W. Tsai, *MRS Bull.* **34**, 485 (2009).

²A. Baraskar, A. C. Gossard, and M. J. W. Rodwell, *J. Appl. Phys.* **114**, 154516 (2013).

³S. J. Pearton, *Int. J. Mod. Phys. B* **7**, 4687 (1993).

⁴M. V. Rao, S. M. Gulwadi, P. E. Thompson, A. Fathimulla, and O. A. Aina, *J. Electron. Mater.* **18**, 131 (1989).

⁵T. Penna, B. Tell, A. S. H. Liao, T. J. Bridges, and G. Burkhardt, *J. Appl. Phys.* **57**, 351 (1985).

⁶C. Carmody, H. H. Tan, and C. Jagadish, *J. Appl. Phys.* **94**, 6616 (2003).

⁷A. G. Lind, M. A. Gill, C. Hatem, and K. S. Jones, *Nucl. Inst. Methods Phys. Res., B* **337**, 7 (2014).

⁸A. G. Lind, N. G. Rudawski, N. J. Vito, C. Hatem, M. C. Ridgway, R. Hengstebeck, B. R. Yates, and K. S. Jones, *Appl. Phys. Lett.* **103**, 232102 (2013).

⁹H. L. Aldridge, A. G. Lind, M. E. Law, C. Hatem, and K. S. Jones, *Appl. Phys. Lett.* **105**, 042113 (2014).

¹⁰D. G. Deppe, N. Holonyak, F. A. Kish, and J. E. Baker, *Appl. Phys. Lett.* **50**, 998 (1987).

¹¹J. J. Murray, M. D. Deal, and D. A. Stevenson, *Appl. Phys. Lett.* **56**, 472 (1990).

¹²W. Walukiewicz, *Phys. Rev. B* **50**, 5221 (1994).

¹³A. Satta, E. Simoen, T. Clarysse, T. Janssens, A. Benedetti, B. De Jaeger, M. Meuris, and W. Vandervorst, *Appl. Phys. Lett.* **87**, 172109 (2005).

¹⁴A. Alian *et al.*, *Microelectron. Eng.* **88**, 155 (2011).

¹⁵K. Y. Cheng, *J. Appl. Phys.* **53**, 4411 (1982).

¹⁶T. Fujii, T. Inata, K. Ishii, and S. Hiyamizu, *Electron. Lett.* **22**, 191 (1986).

¹⁷Y. Fedoryshyn, M. Beck, P. Kaspar, and H. Jaeckel, *J. Appl. Phys.* **107**, 093710 (2010).

¹⁸A. K. Baraskar, M. A. Wistey, V. Jain, U. Singiseti, G. Burek, B. J. Thibeault, Y. J. Lee, A. C. Gossard, and M. J. W. Rodwell, *J. Vac. Sci. Technol. B* **27**, 2036 (2009).

¹⁹J. E. Northrup and S. B. Zhang, *Phys. Rev. B* **47**, 6791 (1993).

²⁰J. Dabrowski and J. E. Northrup, *Phys. Rev. B* **49**, 14286 (1994).

²¹E. Hailemariam, S. J. Pearton, W. S. Hobson, H. S. Luftman, and A. P. Perley, *J. Appl. Phys.* **71**, 215 (1992).

- ²²N. Watanabe, T. Nittono, and K. Watanabe, *Appl. Phys. Lett.* **61**, 1945 (1992).
- ²³W. Walukiewicz, *Appl. Phys. Lett.* **54**, 2094 (1989).
- ²⁴W. Walukiewicz, *Phys. B: Condens. Matter* **302**, 123 (2001).
- ²⁵E. Y. J. Kong, P. Guo, X. Gong, Bin Liu, and Y.-C. Yeo, *IEEE Trans. Electron Devices* **61**, 1039 (2014).
- ²⁶J. C. Ho, R. Yerushalmi, Z. A. Jacobson, Z. Fan, R. L. Alley, and A. Javey, *Nat. Mater.* **7**, 62 (2007).
- ²⁷J. C. Ho *et al.*, *Appl. Phys. Lett.* **95**, 072108 (2009).
- ²⁸U. Singisetti, M. A. Wistey, J. D. Zimmerman, B. J. Thibeault, M. J. W. Rodwell, A. C. Gossard, and S. R. Bank, *Appl. Phys. Lett.* **93**, 183502 (2008).
- ²⁹Y. H. Yeh and J.-T. Lai, *Jpn. J. Appl. Phys.* **35**, L1569 (1996).
- ³⁰G. Stareev, H. Künzel, and G. Dortmann, *J. Appl. Phys.* **74**, 7344 (1993).
- ³¹J. C. Lin, S. Y. Yu, and S. E. Mohny, *J. Appl. Phys.* **114**, 044504 (2013).